Water-Mediated Hydrogen-Bonded Network on the Cytoplasmic Side of the Schiff Base of the L Photointermediate of Bacteriorhodopsin†

Akio Maeda,‡,§ Judith Herzfeld,|| Marina Belenky,|| Richard Needleman,⊥ Robert B. Gennis,‡ Sergei P. Balashov,§,▽ and Thomas G. Ebrey*,§

Department of Biochemistry, University of Illinois at Urbana/Champaign, Urbana, Illinois 61801, Department of Chemistry, Brandeis University, Waltham, Massachusetts 02454, Department of Biochemistry, Wayne State University School of Medicine, Detroit, Michigan 48201, and Department of Biology, University of Washington, Seattle, Washington 98195

Received June 19, 2003; Revised Manuscript Received September 22, 2003

ABSTRACT: The L intermediate in the proton-motive photocycle of bacteriorhodopsin is the starting state for the first proton transfer, from the Schiff base to Asp85, in the formation of the M intermediate. Previous FTIR studies of L have identified unique vibration bands caused by the perturbation of several polar amino acid side chains and several internal water molecules located on the cytoplasmic side of the retinylidene chromophore. In the present FTIR study we describe spectral features of the L intermediate in D_2O in the frequency region which includes the N−D stretching vibrations of the backbone amides. We show that a broad band in the 2220−2080 cm^{-1} region appears in L. By use of appropriate ^{15}N labeling and mutants, the lower frequency side of this band in L is assigned to the amides of Lys216 and Gly220. These amides are coupled to each other, and interact with Thr46 and Val49 in helix B and Asp96 in helix C via weakly H-bonding water molecules that exhibit O−D stretching vibrations at 2621 and 2605 cm^{-1}. These water molecules are part of a hydrogen-bonded network characteristic of L which includes other water molecules located closer to the chromophore that exhibit an O−D stretching vibration at 2589 cm^{-1}. This structure, extending from the Schiff base to the internal proton donor Asp96, stabilizes L and affects the L-to-M transition.

Bacteriorhodopsin carries out light-driven proton transport, from the cytoplasm to the extracellular medium, across the purple membrane. A retinylidene moiety, formed by a Schiff base linkage between retinal and Lys216, is responsible for the absorption of light. The pump cycle starts with the photoinduced isomerization of the all-trans chromophore in the light-adapted initial state (BR[1]) to its 13-cis form. Subsequent changes occur through a series of intermediates: K, L, M, N, and O (*1*). The intermediates can be distinguished by their visible spectra, which reflect changes in the structure of the chromophore and the protein (*2*, *3*). Further characteristic changes for each transition can be sensitively detected by difference FTIR spectroscopy, giving specific information on the protonation states of ionizable residues, interactions of the chromophore with the protein (reviewed in ref *4*) and changes in internal water molecules (reviewed in refs *5* and *6*). Analyses of these spectra have provided important insights into the mechanism of proton pumping.

Hydrogen-bonding of the Schiff base becomes weaker after the primary photoreaction, the BR-to-K transition (*7*, *8*), and stronger again in the K-to-L transition (*7*, *9*). The first proton transfer from the Schiff base to Asp85 occurs in the L-to-M transition (*10*). The lowering of the pK_a of the Schiff base is a primary requirement for the proton transfer to Asp85. Conceptually, before the deprotonation of the Schiff base occurs, a proper environment of Asp85 and a pathway for the transfer must be established. In this respect the protonated Schiff base must be temporarily stabilized in L. The chromophore distortions seen in L may be responsible for the pK_a decrease; they are gone upon reprotonation of the Schiff base in N (*9*, *11*). Though not easily distinguished from the other M's spectroscopically, an M subspecies called M_1 is in equilibrium with L (*12*, *13*). Disruption of the Schiff base−counterion interaction, upon neutralization of both by proton transfer in the L-to-M_1 transition, would allow relaxation of the chromophore distortion of the Schiff base in the transition from M_1 to M_2 and would explain the absence of distortion seen in N. Such relaxation of the chromophore while the Schiff base is deprotonated may be critical in ensuring one-way proton transfer in the photocycle (*14*−*16*).

FTIR studies have shown that many of the structural perturbations characteristic of L occur on the cytoplasmic side of the chromophore (see Figure 1 for BR) (*17*). These include the perturbation of Asp96 (*10*), Asp115 (*10*), and Trp182 (*18*), which are relatively far from the Schiff base (more than 7 Å), as well as Val49 (*19*) and Thr89 (*20*), which

† This work was supported by NIH Grants GM 52023 (to T.G.E. and S.P.B.), GM 36810 (to J.H.), and HL 16101 (to R.B.G.).

* To whom correspondence should be addressed. Phone: (206) 685-3550. Fax: (206) 543-3262. E-mail: tebrey@u.washington.edu.

‡ University of Illinois at Urbana/Champaign.

§ University of Washington.

|| Brandeis University.

⊥ Wayne State University School of Medicine.

▽ Present address: Department of Physiology and Biophysics, University of California, Irvine, CA 92697.

[1] Abbreviations: BR, all-trans bacteriorhodopsin; HOOP, hydrogen out-of-plane.

10.1021/bi0301542 CCC: $25.00
Published on Web 11/12/2003

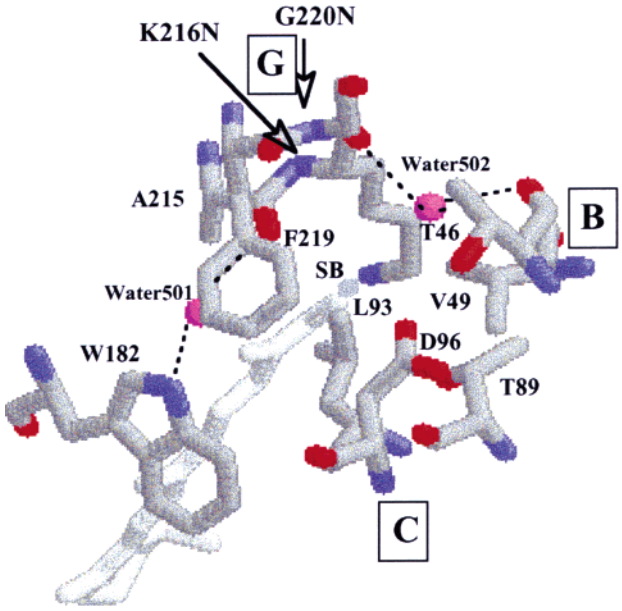

FIGURE 1: View from the cytoplasm of amino acid residues discussed in the present study. All the residues are depicted according to the structure of wild-type BR (1c3w in the Protein Data Bank (*33*)). The picture is tilted so as to avoid overlap of the amides of Gly220 and Lys216. The retinal is shown in pale gray. In helix G, Gly220 and Phe219 are located one turn in the cytoplasmic direction from Lys216 and Ala215, respectively. In helix B, Thr46 is located one turn to the cytoplasmic side from Val49. In helix C, Asp96 is closer to the cytoplasmic surface than Leu93 and Thr89. SB stands for the Schiff base. Two water molecules (Water501 and Water502) are depicted by pink balls connected by dotted lines to H-bonding partners within 3 Å.

are close to the Schiff base. Other changes involve several internal water molecules whose O−H stretching bands appear in the 3650−3450 cm^{-1} region with much larger amplitudes in L than in BR. These frequencies indicate that these water molecules have relatively weak H-bonds. They have been proposed to be involved in shifting the L-to-M equilibrium toward L (*21*, *22*). Location of the waters on the cytoplasmic side is suggested by depletion of these water bands in the T46V mutant (*21*). Further FTIR studies have shown that at least one of these water molecules is close to the Schiff base (*22*) and probably close to the 13-methyl group of the retinylidene chromophore (*23*). In L′, the all-trans photoproduct of L (*24*, *25*), an intense water band at 3589 cm^{-1} in L is preserved with a slight frequency shift to 3549 cm^{-1} (*26*). Also preserved are the perturbations of Asp96, Val49, Lys216, and the methyl group of the retinal that occur in forming L. On the other hand, perturbations of Trp182 and Asp115 which occur in forming L are largely relaxed in L′. These results suggest that the structure from the Schiff base to Asp96, along helices B (including Thr46, which interacts with Asp96 and Val49), C (Asp96), and G (Lys216), is perturbed as a coordinated unit in L.

Following photoisomerization and deprotonation of the Schiff base, the movement of the side chain of Lys216 causes changes in the position of its backbone atoms (*27*). This movement is relatively large in some X-ray structures of M, and the H-bonding between the carbonyl of Lys216 and the amide of Gly220 in helix G is disrupted (see Protein Data Bank entries 1f4z (*28*), 1cwq (*29*), and 1kg9 (*30*)). In these structures a water molecule (Water503) hydrates the amide of Gly220. In two of the structures (1f4z and 1cwq) this water is further connected to Thr46 and Asp96 through another water molecule (Water504). In the third structure (*30*), a cavity with the capacity for one water molecule at the position of Water504 was found. However, in an early M produced by irradiation at 210 K (*16*) and in L (*27*) the movement of backbone atoms is smaller, and water molecules were not detected in these positions. Between the carbonyls of Thr46 and Lys216 the only water molecule present is Water502 as in the initial BR state.

Atomic level structures of bacteriorhodopsin (*31*−*36*) show a rather nonpolar region among Thr46, Asp96, and the Schiff base in the cytoplasmic domain. Side chains of Val49, Leu93, Trp182, and Phe219 constitute the core of this region. It should be noted that, even in a highly nonpolar environment, the amide and carbonyl groups of the peptide backbone provide some polar character, along with H-bonding water molecules. A nonpolar environment will strengthen the interactions of these groups. Difference FTIR spectroscopy is a sensitive technique to detect weakly H-bonding water molecules because the polarization of chemical bonds by electrostatic interactions intensifies the infrared absorption bands. Our recent FTIR studies of the interaction of the Schiff base with water in L (*22*) indicated that the hydrogen out-of-plane (HOOP) vibrations of the Schiff base are intensified by interaction with water. This could also be true for the stretching vibrations of the amide N−D. FTIR spectroscopy would also reveal the amide N−D as a binding site for other water molecules that are involved in stabilization of L.

The K-minus-BR spectrum of bacteriorhodopsin exhibits a broad negative set of bands in the 2800−2500 cm^{-1} region (*37*). In D_2O some of these bands shift and appear as a corresponding broad band in the 2220−2080 cm^{-1} region. In this paper we observe broad difference bands for L in this spectral region and show by the use of mutant pigments and appropriate isotope labeling that they contain a contribution from N−D stretching vibrations of the two amides of Gly220 and Lys216, which are interacting with water molecules and nearby residues, Thr46 and Asp96. We propose that the interaction of water molecules with these amides occurs upon formation of L. This structural change involves several residues extending from the chromophore to Asp96. It plays a role in stabilizing the L state and affects the L-to-M transition.

MATERIALS AND METHODS

Bacteriorhodopsin Samples. Isotopically enriched bacteriorhodopsins were prepared biosynthetically using a growth medium similar to that of Gochnauer and Kushner (*38*) with labeled amino acids replacing their natural counterparts. The concentrations were 0.085 g/L for [α-^{15}N]-labeled L-lysine and 0.06 g/L for [^{15}N]-labeled glycine. The ^{15}N labels are not significantly scrambled to other sites because any nitrogen from degraded amino acids is diluted by a large unlabeled ammonia pool.

Purple membranes of wild-type and mutant pigments were isolated by the standard procedure (*39*). The mutant strains T46V/F219L and G220P were obtained by the procedure of Needleman et al. (*40*). The mutant pigments T46V, T46V/D96N, V49A, D96N, and F219L were kindly donated by J. K. Lanyi and L. S. Brown and described previously (*21*−*23*, *26*, *41*, *42*).

The photoproducts of V49A at 80 K contained about 15% L, as judged from the L-specific band of Trp182 at 3486 cm^{-1} (*43*). Subtraction of 15% of L leaves a K-like spectrum with an intense 1194 cm^{-1} band, though the K-specific intense HOOP band at 951 cm^{-1} is missing. Although the K-minus-BR difference spectrum of G220P had a normal shape, only a small percent of L was formed (~10%), which made the difference spectra quite noisy. Other mutants exhibited nearly normal K-minus-BR and L-minus-BR spectra in the 1800−800 cm^{-1} region. As before (*23*) we used the bands of the chromophore at 1168 and 1009 cm^{-1} to scale the spectral amplitudes for the isotope-labeled samples and mutant pigments.

FTIR Measurements. Preparation of the dried films on BaF_2 windows, hydration, and mounting into the cryostat (Oxford Optistat) were described previously (*22*). In this study, almost all the experiments were done with the films hydrated by D_2O or $D_2{}^{18}O$ (ICON, 85.5% ^{18}O, 80% D). Although the membranes were not washed in D_2O, the exchangeable protons were nearly completely replaced with deuterons, as judged by the intensity of the 3642 cm^{-1} O−H stretching vibration of an internal water molecule.

The hydrated films were illuminated in the cryostat, which had been installed in the FTIR spectrometer (BioRad FTS6000). After light-adapting for 5 min at 273 K with yellow light (wavelength >450 nm) obtained from a projector lamp with a Corning 3-72 filter, the sample was cooled to 80 K. Absolute spectra (average of eight spectra, each of which comprised 256 scans at 2 cm^{-1} resolution) were recorded at 80 K before (A) and after (B) illumination with blue light (Corning 4-96 filter, 350−500 nm) for 1 min to form K. The sample was then warmed to 170 K (in ~7 min), held for 10 min to convert K to L, and then recooled to 80 K (in ~14 min) to record further absolute spectra (C). The warming procedure for the hydrated films in the present FTIR study, in contrast to the previous visible spectroscopic studies for the water-glycerol suspensions (*3*), gave complete conversion of K to L, as judged by the elimination of the K-specific bands at 1296 and 951 cm^{-1} and the preservation of the BR bands at 1168 and 1009 cm^{-1} as described previously for the wild-type and other mutant pigments (*23*). The L-minus-BR spectrum thus obtained is also free from M as judged from the lack of the M-specific bands at 1750, 1565, and 1554 cm^{-1} (see the review in ref *4*). The K-minus-BR and L-minus-BR difference spectra at 80 K are given by (B) − (A) and (C) − (A), respectively. In this way we can compare L as the thermal product of K in the same hydrated film at the same temperature.

After these recordings, the sample was warmed to 273 K before the next cycle of measurements at low temperatures. The measurements were repeated at least three times, and the data were averaged. The reproducibility of all the presented data was confirmed by two independent sets of experiments.

RESULTS

The L Intermediate Exhibits a Set of Bands in the 2200−2080 cm^{-1} Region in D_2O. Figure 2 shows K-minus-BR, L-minus-BR, and L-minus-K spectra in the 2230−1770 cm^{-1} region at 80 K for a film hydrated with D_2O. The negative portion of the difference spectrum, due to BR, exhibits

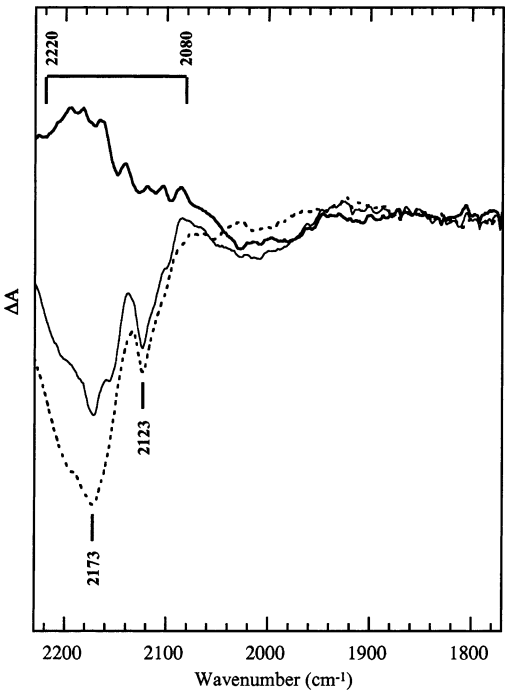

FIGURE 2: Spectra for wild-type bacteriorhodopsin in D_2O: K-minus-BR (dotted line) and L-minus-BR (thin line) spectra recorded at 80 K and L-minus-K spectrum obtained by subtracting these two spectra (thick line). The full length of the ordinate corresponds to 0.0069 absorbance unit for unlabeled bacteriorhodopsin.

minima at 2173 and 2123 cm^{-1}, as described by Kandori et al. (*37*). To make an accurate comparison between the K-minus-BR and L-minus-BR difference spectra, the spectra should be measured at the same temperature for the same hydrated film. The L-minus-BR spectrum was obtained at 80 K by subtracting the absolute spectrum at 80 K before illumination from the absolute spectrum of the sample that was illuminated at 80 K, warmed to 170 K, and then held for 10 min before recooling to 80 K (see the Materials and Methods). The L-minus-BR spectrum in the 2230−1770 cm^{-1} region (thin line) recorded at 80 K exhibited a smaller negative amplitude than the K-minus-BR spectrum (dotted line). This result indicates that L has a new positive band overlapping the negative bands of BR at 2173 and 2123 cm^{-1}, and reducing their amplitude. In the L-minus-K spectrum (thick line), obtained by subtracting the K-minus-BR spectrum from the L-minus-BR spectrum, this band can be clearly seen as a broad positive band ranging from 2220 to 2080 cm^{-1} with a number of subbands. Frequencies above 2230 cm^{-1} will not be discussed because of strong absorption by D_2O.

A comparison of the L-minus-BR and K-minus-BR spectra in this region was reported recently by Tanimoto et al. (*44*). In their study, the negative bands in the L-minus-BR spectrum were less intense than in the K-minus-BR spectrum, and did not shift in [^{18}O]water, although [^{18}O]water did cause a shift to lower frequency of the 2173 cm^{-1} band of BR in the K-minus-BR spectrum (*45*). From these results, Tanimoto et al. (*44*) argued that the water O−D stretching vibration band at 2173 cm^{-1} in BR returned in L to the frequency it was initially at in BR. However, the shift of the 2173 cm^{-1} band in the K-minus-BR spectrum by $D_2{}^{18}O$ was much smaller than the expected shift for an O−D vibration (~13 cm^{-1}) in this spectral range. Moreover, the L-minus-BR

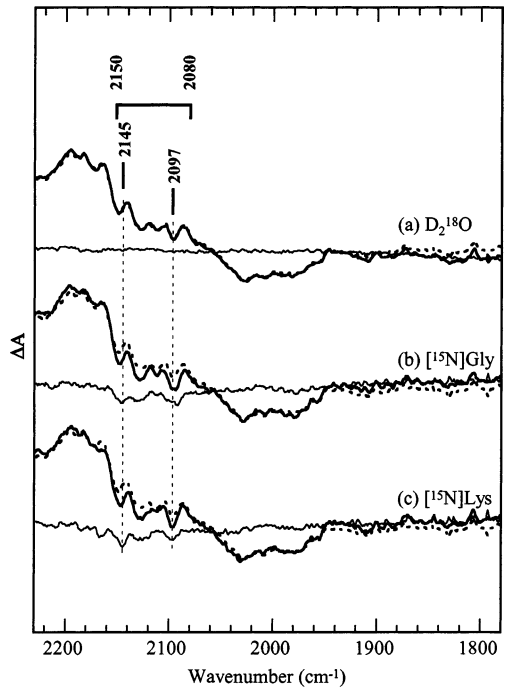

FIGURE 3: Effects of substitution of D_2O by $D_2{}^{18}O$ (a) and isotope labeling in [^{15}N]Gly-labeled bacteriorhodopsin (b) and [α-^{15}N]Lys-labeled bacteriorhodopsin (c) on the L-minus-K spectrum in D_2O. The spectrum of the unlabeled bacteriorhodopsin in D_2O (duplicated from Figure 2a) is superimposed by dotted lines. The differences between the spectrum of the unlabeled sample in D_2O and $D_2{}^{18}O$ (a) and the spectrum of the unlabeled sample and each labeled sample (b, c) are shown by thin lines. The full length of the ordinate corresponds to 0.0069 absorbance unit for unlabeled bacteriorhodopsin.

spectrum was obtained at a different temperature from that for the K-minus-BR spectrum. In our study, L was produced thermally from K and the L-minus-BR spectrum was recorded at the same temperature as that for the K-minus-BR spectrum. We observed no effect of $D_2{}^{18}O$ water substitution on the spectrum of L in this region (see the positive side of the L-minus-K spectrum (Figure 3a).

Interaction of the Amides of Gly220 and Lys216 with Each Other in L. The 2220−2080 cm^{-1} band of the L-minus-K spectrum probably has contributions from the N−D stretching vibrations of backbone amides and the Schiff base N−D. These are the most likely candidates for bands in this spectral region. Moreover, the N−D stretching vibration of the Schiff base of BR has been assigned to bands right in this region (2173 and 2123 cm^{-1} bands in the K-minus-BR spectrum) (*8*). The 2230−1780 cm^{-1} region of the L-minus-K spectra of [^{15}N]Gly-labeled bacteriorhodopsin (Figure 3b) and [α-^{15}N]Lys-labeled bacteriorhodopsin (Figure 3c) are compared with that of unlabeled bacteriorhodopsin (dotted lines). These isotope substitutions consistently lowered the intensity in the 2150−2080 cm^{-1} region. To see the isotope effect more clearly, the difference between the spectra of the unlabeled bacteriorhodopsin and each ^{15}N-labeled bacteriorhodopsin was calculated (thin lines). Though noisy, distinct depletion bands with similar amplitudes were seen at around 2145 and 2097 cm^{-1} for isotopic substitution at the two different N positions. Heavy isotope substitution in the group responsible for a vibration generally causes a shift to lower frequencies and often decreases the intensity of the band. These bands could arise from transition dipole coupling if the dipoles of two Gly/Lys amides with similar vibrational frequencies are located near each other and are nearly parallel (*46*, *47*). The shift in frequency due to ^{15}N substitution in one of these amides should weaken the vibration coupling and cause attenuation in the intensity of the coupled bands.

An obvious Gly−Lys pair is on helix G. The N−D of Gly220 is located at about one α-helical turn from the N−D of Lys216 (see Figure 1). Thus, the two bands of L that were depleted at 2145 and 2097 cm^{-1} are likely at least partly due to the amides of Lys216 and Gly220. No clear changes in intensity in [ζ-^{15}N]Lys-labeled bacteriorhodopsin were detected in any part of this band (data not shown), though greater noise for this sample hampered the detection of possible smaller changes.

Effects of Mutations of Thr46, Val49, Asp96, Phe219, and Gly220 on the Broad Band at 2220−2080 cm^{-1} in L. It is known that several residues around these amides affect the water O−H stretching bands in the 3550−3450 cm^{-1} region of L. These bands are depleted in T46V, partially restored in T46V/D96N, and increased in V49A (*19*, *21*). In D_2O, F219L exhibited a larger water O−D stretching band at 2589 cm^{-1} in L (ref *23*; see also Figure 6).

The F219L mutation also affects the water O−H band at 3671 cm^{-1} of M (*42*). Among the residues which affect the water vibrations in BR, Thr46, Asp96, and Phe219 are close to the amide of Gly220, and Val49 is close to that of Lys216 (Figure 1), but not directly in contact with the amides. These relations probably will also hold for L since the structures of BR and L are fairly similar (*27*, *48*). To know the relationship of these residues to the 2220−2080 cm^{-1} band, we examined the L-minus-K spectra of the mutants T46V, T46V/D96N, V49A, D96N, F219L, T46V/F219L, and G220P.

The spectra of mutants in Figure 4 (T46V (a), F219L (b), T46V/F219L (c), and G220P (d)) show decreased intensities in the 2200−2080 cm^{-1} region. At the same time, a broad band appears in the 2030−1780 cm^{-1} region for T46V and F219L. This suggests that the broad band at 2200−2080 cm^{-1} shifts to the 2030−1780 cm^{-1} region in F219L (b). The latter band becomes less intense with an additional mutation of T46V in T46V/F219L (c), as in T46V (a). Abolition of the broad band in G220P (d), which does not have an N−D group at position 220, is consistent with the interpretation that this band arises from the Gly220 amide. The results in Figure 5 for mutants, V49A (a), D96N (b), and T46V/D96N (c), also show decreased intensities in the 2200−2080 cm^{-1} region, but to a lesser extent than in Figure 4, except for the region of 2097 cm^{-1}. It should be noted that the band intensity that was lost in T46V (broken line in Figure 5b,c) is partially restored by the additional mutation of D96N in T46V/D96N (solid line in Figure 5c), exhibiting the same level as in D96N (solid line in Figure 5b). Taken together, the results indicate that the coupled vibration mode of the peptide N−D's of Lys216 and Gly220 are perturbed by mutations of Thr46, Phe219, Gly220, Val49, and Asp96. The first three depleted the bands more extensively than the latter two.

Effects of Mutations of Thr46, Val49, Asp96, and Phe219 on the Water O−D Vibrations. We expect that the effects of these mutations on the amide vibration bands of L are due to their effect on the waters between the side chains of the mutated residues and the amides of Lys216 and Gly220.

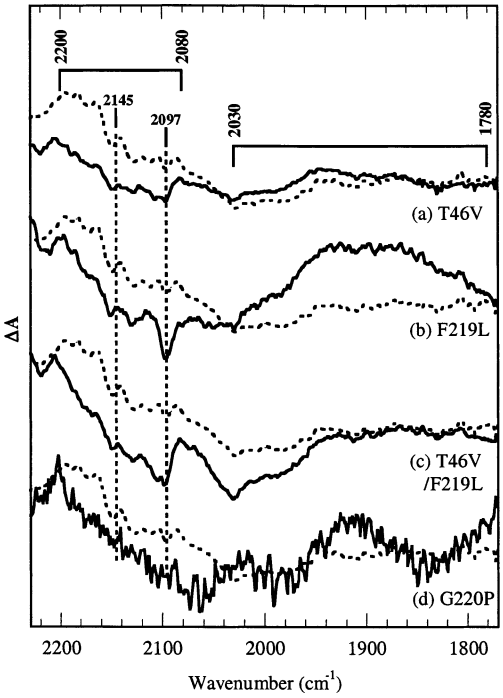

FIGURE 4: Effects of mutations on the L-minus-K spectrum in D_2O. Solid lines show spectra of mutant pigments: T46V (a), F219L (b), T46V/F219L (c), and G220P (d). Dotted lines show the spectrum of wild-type bacteriorhodopsin (duplicated from the thick line in Figure 2). The frequencies at 2145 and 2097 cm^{-1} are marked by vertical dotted lines. The full length of the ordinate corresponds to 0.0083 absorbance unit for unlabeled bacteriorhodopsin.

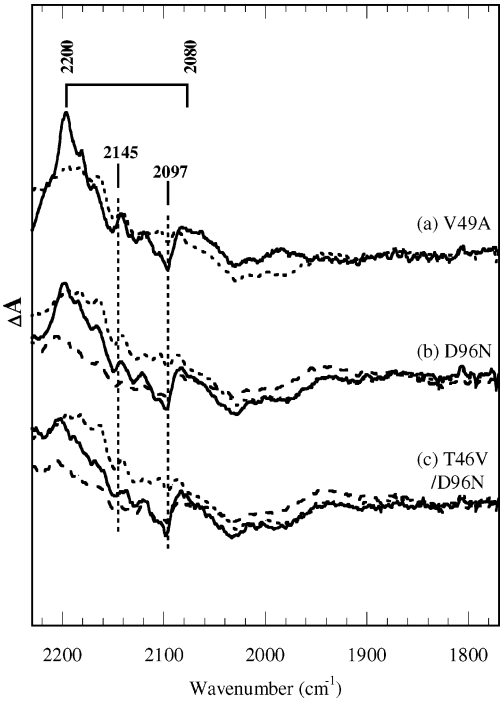

FIGURE 5: Effects of mutations on the L-minus-K spectrum in D_2O. Solid lines show spectra of mutant pigments: V49A (a), D96N (b), and T46V/D96N (c). Dotted lines show the spectrum of wild-type bacteriorhodopsin (duplicated from the thick line in Figure 2), and broken lines show the spectrum of T46V (reproduced from Figure 4a). The frequencies at 2145 and 2097 cm^{-1} are marked by vertical dotted lines. The full length of the ordinate corresponds to 0.0083 absorbance unit for unlabeled bacteriorhodopsin.

Figure 6 shows the spectra of several mutants in the 2700−2550 cm^{-1} region where the water O−D vibrations of L are seen (*23*). The water O−D stretching vibrations are detected as bands which undergo a shift of ∼16 cm^{-1} when transferred from D_2O to $D_2{}^{18}O$ (thin lines). The spectrum of each mutant is compared with that of the wild type (dotted lines). The water O−H stretching vibrations of T46V, T46V/D96N, and V49A have been reported previously (*19*, *21*). However, in D_2O the effects on the water bands can be evaluated more clearly without interference from an overlapping band at 3486 cm^{-1} (*43*), which was not shifted to the O−D stretching region. The O−D stretching bands of the wild type and F219L, reported previously (*23*), are duplicated here for comparison with the other mutants.

The water O−D stretching bands of L for the wild type (dotted lines in Figure 6) appear at 2621, 2605, and 2589 cm^{-1} (*23*). Among them the 2621 cm^{-1} band is virtually absent in T46V (a), F219L (b), and T46V/F219L (c). On the other hand, this band is almost unchanged in the other mutants, V49A (d), D96N (e), and T46V/D96N (f), albeit with a shift to lower frequencies in V49A and some broadening toward lower frequencies in D96N and T46V/D96N. The 2605 cm^{-1} band is also eliminated completely by T46V (a) and T46V/F219L (c) mutations. This band is diminished or shifted toward lower frequencies in F219L (b) and V49A (d). These effects of the mutants on the 2621 and 2605 cm^{-1} bands correlate with their above-described effects on the broad 2200−2080 cm^{-1} band of L. The T46V, F219L, and T46V/F219L mutants caused larger depletion of this band (Figure 4) with the concomitant appearance of the 2030−1780 cm^{-1} band, while V49A, D96N, and T46V/D96N mutants mainly affected the 2097 cm^{-1} band (Figure 5). We propose that the water molecules responsible for the 2621 and 2605 cm^{-1} bands are probably involved in the

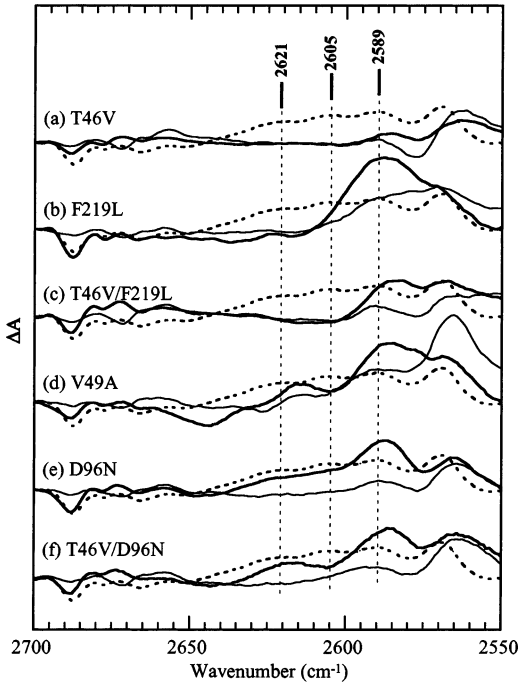

FIGURE 6: Effects on the water O−D stretching bands in the L-minus-BR spectrum in D_2O of mutations T46V (a), F219L (b), T46V/F219L (c), V49A (d), D96N (e), and T46V/D96N (f). The corresponding spectrum in $D_2{}^{18}O$ is superimposed by thin lines. The spectrum of wild-type bacteriorhodopsin hydrated by D_2O is superimposed by dotted lines. The full length of the ordinate corresponds to 0.035 absorbance unit for wild-type bacteriorhodopsin.

interaction of the side chains of Thr46 and Asp96 with the amides of Lys216 and Gly220.

The intense water bands at 2589 and 2605 cm^{-1} of the wild type changed to an intense band at 2629 cm^{-1} in the L-to-L′ conversion and were suggested to be involved in the stabilization of L relative to K (*23*). In contrast to its effect on the 2621 and 2605 cm^{-1} water bands, the T46V mutation retained the 2589 cm^{-1} band, though with a reduced intensity and with a shift to lower frequencies. Other mutants, F219L (b), V49A (d), and D96N (e), rather intensify this band on the lower frequency side. Finally it should be noted that the intensities of the water O−D bands that were eliminated or reduced in T46V (a) were restored in T46V/D96N (f) to the level that was observed in D96N (e).

DISCUSSION

A H-Bonding Network in L Is Formed around the Gly220−Lys216 Amides. The broad band in the 2220−2080 cm^{-1} region of L could be due to a Fermi resonance (*49*), which produces multiple bands by the coupling of similar vibrational modes including the overtones and combination of amides and water. In this case we would expect a shift upon $D_2{}^{18}O$ substitution, but this shift is not observed (Figure 3a). An alternative explanation is to regard the broad band as a continuum band. The idea of a continuum band was proposed by Zundel (*50*), who showed that such a band may arise by proton delocalization in a H-bonded network between H-bonding partners. This band should be located between the frequencies of the partners. This mechanism might be operative in a water-mediated H-bonding network around the amides of Gly220 and Lys216 in L. Vibrations due to the amides of Gly220 and Lys216 were detected on the lower frequency side of the 2220−2080 cm^{-1} band (Figure 3), and these amides are taken to be partners in forming the H-bonded network. Water molecules responsible for the O−D stretching vibration at 2621 and 2605 cm^{-1}, which were depleted together with the wide 2220−2080 cm^{-1} band in T46V and F219L (Figures 4 and 6), probably provide the bridge between the partners. At first, the effects of T46V and D96N mutations led us to consider the O−D stretching vibrations of Thr46 and Asp96 as candidates for the partners that are on the higher frequency side of the band. However, these O−D stretching vibrations are not likely to be present in this frequency region (*20*). Another candidate is the N−D stretching vibration of the Schiff base, which might be present in this region. Though not identified by clear isotope shifts, it is expected to be at lower frequencies than the corresponding N−D vibrations of K, 2495 and 2468 cm^{-1} (*8*), because of stronger H-bonding. If this is so, the broad band could arise from a H-bonding network between the Lys216/Gly220 amides and the Schiff base. The perturbing effects of T46V and D96N mutations could be due to interactions of intervening water molecules with Thr46 and Asp96. The interaction of water molecules on the cytoplasmic side with the Schiff base has previously been suggested (*22*). The present study suggests the presence of water molecules, one with the O−D stretching vibrations at 2621 and 2605 cm^{-1} between Thr46−Asp96 and the backbone amides of Lys216−Gly220, and the other with the vibrations at 2589 cm^{-1} close to the Schiff base. These water molecules may interact with each other.

The recently published X-ray structure of L (*27*) shows that almost all the residues on the cytoplasmic side of the Schiff base stay at nearly the same positions as in the initial unphotolyzed state (see Figure 1). Water502 remains between the carbonyl groups of Thr46 and Lys216, and Water501 stays at the same place between the C═O of Ala215 and the indole N−H of Trp182. These sites are far from the amides of Phe219 and Gly220 where the water with the 2621 and 2605 cm^{-1} bands is proposed to be and far from the Schiff base for the water with the 2589 cm^{-1} band (*22*). Most likely, the additional water molecules responsible for these water vibrations of L form a H-bonding network together with Water502. The X-ray structure did not reveal any of these additional water molecules on the cytoplasmic side of the Schiff base. One possible reason for the discrepancy is that a disordered water molecule with only weak H-bonding might not be detected by X-ray analysis even at high resolution. An example of such a water was shown recently for human interleukin 1β (*51*). These water molecules might not be detected also because of damage to the sample by X-rays; such damage has been shown in acquiring data for K (*52*) and for M (*30*) structures. Alternatively, the apparent differences could arise from an indirect effect of the mutants on the vibration bands. However, this seems less likely. Thus, the location of waters upon L formation inferred from the FTIR data cannot be explained from the current X-ray results, and should be addressed in future studies.

A H-Bonding Network of Water between Asp96 and the Schiff Base Stabilizes L. The D96N mutation in T46V/D96N restores the 2200−2080 cm^{-1} band, which was depleted in T46V, to the level that D96N exhibits (Figure 5). This occurs in parallel with attenuation and restoration of the water O−D stretching vibrations at 2589, 2605, and 2621 cm^{-1} (Figure 6). Similar effects in L were previously observed for the intensities of the carbonyl vibration of Val49 (*19*) and the HOOP vibration of the Schiff base (*22*). More importantly, the T46V mutation shifted the L-to-M equilibrium toward M, and the additional mutation in T46V/D96N partially reversed this (*21*). We proposed that the interaction of the Schiff base with the water molecules affected by the T46V and D96N mutations stabilizes the L state (*22*). The present results suggest that the interaction of the water molecules with the amides of helix G is also involved in the stabilization of the L intermediate. In this context, the role of D96N in T46V/D96N is interesting. Probably, the side chain amide of Asn96 provides a water-binding site that substitutes for the hydroxyl group of Thr46. Hydration of the Asn96 amide by Water504 has been observed by X-ray crystallography of the D96N mutant (*53*).

Earlier we showed that light-induced isomerization of the chromophore, leading to L, perturbs a site which includes the Schiff base, Leu93, and Trp182, and that this structure is temporarily stabilized by rearranged H-bonding of water (giving rise to the 2589 cm^{-1} band) (*23*). The isomerization also causes a slight movement of the side chain of Lys216, which then perturbs the backbone of helix G in the Lys216 to Gly220 region (*27*). This structural change may allow water molecules to fill possible cavities between the amide N−H's of Gly220−Lys216 of helix G and the side chains of Val49, Thr46, and Asp96 in helices B and C (giving rise to the 2621 cm^{-1} band). The residues surrounding the water molecules make a structure unit that may stabilize the L

structure. The water O−D vibration at 2621 cm^{-1} is due to water with relatively weak H-bonding. Such weakly H-bonding waters are probably the best candidates for the water molecules filling cavities in the otherwise tight protein matrix of L. We propose that the interaction of the backbone amides of helix G (Lys216 and Gly220) with the weak H-bonding water molecules leads to the formation of a H-bonding network extending from the Schiff base to the internal proton donor Asp96 that is involved in L formation and affects the L-to-M transition.

ACKNOWLEDGMENT

We are thankful to Dr. Joel E. Morgan for his invaluable help in maintaining the FTIR facilities.

REFERENCES

1. Lozier, R. H., Bogomolni, R. A., and Stoeckenius, W. (1975) Bacteriorhodopsin: A light-driven proton pump in *Halobacterium halobium*, *Biophys. J. 15*, 955−963.
2. Lanyi, J. K., and Váró, G. (1995) The photocycles of bacteriorhodopsin, *Isr. J. Chem. 35*, 365−385.
3. Balashov, S. P., and Ebrey, T. G. (2001) Trapping and spectroscopic identification of the photointermediates of bacteriorhodopsin at low temperatures, *Photochem. Photobiol. 73*, 453−462.
4. Maeda, A. (1995) Application of FTIR spectroscopy to the structural study on the function of bacteriorhodopsin, *Isr. J. Chem. 35*, 387−400.
5. Kandori, H. (2000) Role of internal water molecules in bacteriorhodopsin, *Biochim. Biophys. Acta 1460*, 177−191.
6. Maeda, A. (2001) Internal water molecules as mobile polar groups for light-induced proton translocation in bacteriorhodopsin and rhodopsin as studied by difference FTIR spectroscopy, *Biochemistry (Moscow) 66*, 1555−1569.
7. Maeda, A., Sasaki, J., Pfefferlé, J.-M., Shichida, Y., and Yoshizawa, T. (1991) Fourier transform infrared spectral studies on the Schiff base mode of all-trans bacteriorhodopsin and its photointermediates, *Photochem. Photobiol. 54*, 911−921.
8. Kandori, H., Belenky, M., and Herzfeld, J. (2002) Vibrational frequency and dipolar orientation of the protonated Schiff base in bacteriorhodopsin before and after photoisomerization, *Biochemistry 41*, 6026−6031.
9. Hu, J. G., Sun, B. Q., Petkova, A. T., Griffin, R. G., and Herzfeld, J. (1997) The predischarge chromophore in bacteriorhodopsin: A ^{15}N solid-state NMR study of the L photointermediate, *Biochemistry 36*, 9316−9322.
10. Braiman, M. S., Mogi, T., Marti, M., Stern, L. J., Khorana, H. G., and Rothschild, K. J. (1988) Vibrational spectroscopy of bacteriorhodopsin mutants: Light-driven proton transport involves protonation changes of aspartic acid residues 85, 96, and 212, *Biochemistry 27*, 8516−8520.
11. Pfefferlé, J.-M., Maeda, A., Sasaki, J., and Yoshizawa, T. (1991) Fourier transform infrared study of the N intermediate of bacteriorhodopsin, *Biochemistry 30*, 6548−6556.
12. Váró, G., and Lanyi, J. K. (1991) Thermodynamics and energy coupling in the bacteriorhodopsin photocycle, *Biochemistry 30*, 5016−5022.
13. Zimányi, L., Váró, G., Chang, M., Ni, B., Needleman, R., and Lanyi, J. K. (1992) Pathways of proton release in the bacteriorhodopsin photocycle, *Biochemistry 31*, 8535−8543.
14. Herzfeld, J., and Tounge, B. (2000) NMR probes of vectoriality in the proton-motive photocycle of bacteriorhodopsin: evidence for an "electrostatic steering" mechanism, *Biochim. Biophys. Acta 1460*, 95−105.
15. Herzfeld, J., and Lansing, J. C. (2002) Magnetic resonance studies of the bacteriorhodopsin pump cycle, *Annu. Rev. Biophys. Biomol. Struct. 31*, 73−95.
16. Lanyi, J., and Schobert, B. (2002) Crystallographic structure of the retinal and the protein after deprotonation of the Schiff base: the switch in the bacteriorhodopsin photocycle, *J. Mol. Biol. 321*, 727−737.
17. Maeda, A., Kandori, H., Yamazaki, Y., Nishimura, S., Hatanaka, M., Chon, Y.-S., Sasaki, J., Needleman, R., and Lanyi, J. K. (1997) Intramembrane signaling mediated by hydrogen-bonding of water and carboxyl groups in bacteriorhodopsin and rhodopsin, *J. Biochem. 121*, 399−406.
18. Yamazaki, Y., Sasaki, J., Hatanaka, M., Kandori, H., Maeda, A., Needleman, R., Shinada, T., Yoshihara, K., Brown, L. S., and Lanyi, J. K. (1995) Interaction of tryptophan-182 with the retinal 9-methyl group in the L intermediate of bacteriorhodopsin, *Biochemistry 34*, 577−582.
19. Yamazaki, Y., Tuzi, S., Saitô, H., Kandori, H., Needleman, R., Lanyi, J. K., and Maeda, A. (1996) Hydrogen bonds of water and C═O groups coordinate long-range structural changes in the L photointermediate of bacteriorhodopsin, *Biochemistry 35*, 4063−4068.
20. Kandori, H., Yamazaki, Y., Shichida, Y., Raap, J., Lugtenburg, J., Belenky, M., and Herzfeld, J. (2001) Tight Asp-85-Thr-89 association during the pump switch of bacteriorhodopsin, *Proc. Natl. Acad. Sci. U.S.A. 98*, 1571−1576.
21. Yamazaki, Y., Hatanaka, M., Kandori, H., Sasaki, J., Karstens, W. F. J., Raap, J., Lugtenburg, J., Bizounok, M., Herzfeld, J., Needleman, R., Lanyi, J. K., and Maeda, A. (1995) Water structural changes at the proton uptake site (the Thr46-Asp96 domain) in the L intermediate of bacteriorhodopsin, *Biochemistry 34*, 7088−7093.
22. Maeda, A., Balashov, S. P., Lugtenburg, J., Verhoeven, M. A., Herzfeld, J., Belenky, M., Gennis, R. B., Tomson, F. L., and Ebrey, T. G. (2002) Interaction of internal water molecules with the Schiff base in the L intermediate of the bacteriorhodopsin photocycle, *Biochemistry 41*, 3803−3809.
23. Maeda, A., Tomson, F. L., Gennis, R. B., Balashov, S. P., and Ebrey, T. G. (2003) Water molecule rearrangements around Leu93 and Trp182 in the formation of the L intermediate in bacteriorhodopsin's photocycle, *Biochemistry 42*, 2535−2541.
24. Litvin, F. F., and Balashov, S. P. (1977) New intermediates in the photochemical conversions of bacteriorhodopsin, *Biophysics 22*, 1157−1160.
25. Hurley, J. B., Becher, B., and Ebrey, T. G. (1978) More evidence that light isomerizes the chromophore of purple membrane protein, *Nature 272*, 87−88.
26. Maeda, A., Tomson, F. L., Gennis, R. B., Ebrey, T. G., and Balashov, S. P. (1999) Chromophore-protein-water interactions in the L intermediate of bacteriorhodopsin: FTIR study of the photoreaction of L at 80 K, *Biochemistry 38*, 8800−8807.
27. Lanyi, J. K., and Schobert, B. (2003) Mechanism of proton transport in bacteriorhodopsin from crystallographic structures of the K, L, M_1, M_2, and M_2' intermediates of the photocycle, *J. Mol. Biol. 328*, 439−450.
28. Luecke, H., Schobert, B., Cartailler, J.-P., Richter, H.-T., Rosengarth, A., Needleman, R., and Lanyi, J. K. (2000) Coupling photoisomerization of retinal to directional transport in bacteriorhodopsin, *J. Mol. Biol. 300*, 1237−1255.
29. Sass, H. J., Büldt, G., Gessenich, R., Hehn, D., Neff, D., Schlesinger, R., Berendzen, J., and Ormos, P. (2000) Structural alterations for proton translocation in the M state of wild-type bacteriorhodopsin, *Nature 406*, 649−653.
30. Facciotti, M. T., Rouhani, S., Burkard, F. T., Betancourt, F. M., Downing, K. H., Rose, R. B., McDermott, G., and Glaeser, R. M. (2001) Structure of an early intermediate in the M-state phase of the bacteriorhodopsin photocycle, *Biophys. J. 81*, 3442−3455.
31. Grigorieff, N., Ceska, T. A., Downing, K. H., Baldwin, J. M., and Henderson, R. (1996) Electron-crystallographic refinement of the structure of bacteriorhodopsin, *J. Mol. Biol. 259*, 393−421.
32. Luecke, H., Richter, H.-T., and Lanyi, J. K. (1998) Proton-transfer pathways in bacteriorhodopsin at 2.3 Angstrom resolution, *Science 280*, 1934−1937.
33. Luecke, H., Schobert, B., Richter, H.-T., Cartailler, J.-P., and Lanyi, J. K. (1999) Structure of bacteriorhodopsin at 1.55 Å resolution, *J. Mol. Biol. 291*, 899−911.
34. Essen, L.-O., Siegert, R., Lehmann, W. D., and Oesterhelt, D. (1998) Lipid patches in membrane protein oligomeres: Crystal structure of the bacteriorhodopsin-lipid complex, *Proc. Natl. Acad. Sci. U.S.A. 95*, 11673−11678.
35. Belrhali, H., Nollert, P., Royant, A., Menzel, C., Rosenbusch, J. P., Landau, E. M., and Pebay-Peyroula, E. (1999) Protein, lipid and water organization in bacteriorhodopsin crystals: a molecular view of the purple membrane at 1.9 Å resolution, *Structure 7*, 909−917.
36. Mitsuoka, K., Hirai, T., Murata, K., Miyazawa, A., Kidera, A., Kimura, Y., and Fujiyoshi, Y. (1999) The structure of bacterior-

hodopsin at 3.0 Å resolution based on electron crystallography: implication of the charge distribution, *J. Mol. Biol. 286*, 861−882.
37. Kandori, H., Kinoshita, N., Shichida, Y., and Maeda, A. (1998) Protein structural changes in bacteriorhodopsin upon photoisomerization as revealed by polarized FTIR spectroscopy, *J. Phys. Chem. B 102*, 7899−7905.
38. Gochnauer, M. B., and Kushner, D. J. (1969) Growth and nutrition of extremely halophilic bacteria, *Can. J. Microbiol. 15*, 1157−1165.
39. Oesterhelt, D., and Stoeckenius, W. (1974) Isolation of the cell membrane of *Halobacterium halobium* and its fractionation into red and purple membrane, *Methods Enzymol. 31*, 667−678.
40. Needleman, R., Chang, M., Ni, B., Váró, G., Fornés, J., White, S. H., and Lanyi, J. K. (1991) Properties of Asp212-Asn bacteriorhodopsin suggest that Asp212 and Asp85 both participate in a counterion and proton acceptor complex near the Schiff base, *J. Biol. Chem. 266*, 11478−11484.
41. Brown, L. S., Yamazaki, Y., Maeda, A., Sun, L., Needleman, R., and Lanyi, J. K. (1994) The proton transfers in the cytoplasmic domain of bacteriorhodopsin are facilitated by a cluster of interacting residues, *J. Mol. Biol. 239*, 401−414.
42. Yamazaki, Y., Kandori, H., Needleman, R., Lanyi, J. K., and Maeda, A. (1998) Interaction of the protonated Schiff base with the peptide backbone of valine 49 and the intervening water molecule in the N photointermediate of bacteriorhodopsin, *Biochemistry 37*, 1559−1564.
43. Maeda, A., Sasaki, J., Ohkita, Y. J., Simpson, M., and Herzfeld, J. (1992) Tryptophan perturbation in the L intermediate of bacteriorhodopsin: Fourier transform infrared analysis with indole-^{15}N shift, *Biochemistry 3*, 12543−12545.
44. Tanimoto, T., Furutani, Y., and Kandori, H. (2003) Structural changes of water in the Schiff base region of bacteriorhodopsin: proposal of a hydration switch model, *Biochemistry 42*, 2300−2306.
45. Kandori, H., and Shichida, Y. (2000) Direct observation of the bridged water stretching vibrations inside a protein, *J. Am. Chem. Soc. 122*, 11745−11746.
46. Krimm, S., and Abe, Y. (1972) Intermolecular interaction effects in the amide I vibrations of polypeptides, *Proc. Natl. Acad. Sci. U.S.A. 69*, 2788−2792.
47. Torii, H. (1999) Liquid structures and the infrared and isotropic/anisotropic Raman noncoincidence in liquid methanol, a methanol-LiCl solution, and a solvated electron in methanol: Molecular dynamics and ab initio molecular orbital studies, *J. Phys. Chem. A 103*, 2843−2850.
48. Hendrickson, F. M., Burkard, F., and Glaeser, R. M. (1998) Structural characterization of the L-to-M transition of the bacteriorhodopsin photocycle, *Biophys. J. 75*, 1446−1454.
49. Vinogradov, S. N., and Linnell, R. H. (1971) *Hydrogen bonding*, Van Norstrand Reinhold Co., New York.
50. Zundel, G. (2000) Hydrogen bonds with large proton polarizability and proton-transfer processes in electrochemistry and biology, *Adv. Chem. Phys. 111*, 1−217.
51. Yu, B., Blaber, M., Gronenborn, A. M., Clore, G. M., and Caspar, D. L. (1999) Disordered water within a hydrophobic protein cavity visualized by X-ray crystallography, *Proc. Natl. Acad. Sci. U.S.A. 96*, 103−108.
52. Matsui, Y., Sakai, K., Murakami, M., Shiro, Y., Adachi, S., Okumura, H., and Kouyama, T. (2002) Specific damage induced by X-ray radiation and structural changes in the primary photoreaction of bacteriorhodopsin, *J. Mol. Biol. 324*, 469−481.
53. Luecke, H., Schobert, B., Richter, H.-T., Cartailler, J.-P., and Lanyi, J. K. (1999) Structural changes in bacteriorhodopsin during ion transport at 2 Angstrom resolution, *Science 286*, 255−260.

BI0301542